



Research article

An experimental and mechanism study on the regioselective click reaction toward the synthesis of thiazolidinone-triazole

Mahdiah Darroudi^a, Mahshid Hamzehloueian^b, Yaghoub Sarrafi^{a,*}^a Department of Organic Chemistry, Faculty of Chemistry, University of Mazandaran, 47416 Babolsar, Iran^b Department of Chemistry, Joluybar Branch, Islamic Azad University, Joluybar, Iran

ARTICLE INFO

Keywords:

Novel triazoles
Thiazolidinone
Click reaction
Mechanism
DFT
ELF

ABSTRACT

An efficient procedure for the synthesis of novel thiazolidinone triazoles through 32 cycloaddition reactions in the presence of copper(I) species was described, and the molecular mechanism of this 32CA was investigated computationally. Different possible pathways for CA process have been studied to achieve this goal, including *one-step* pathways for both regioisomers 1,4- and 1,5-triazoles (uncatalyzed, mono-copper, di-copper) and also mono- and di-copper stepwise pathways for 1,4-disubstituted triazole. It was exhibited that the most convenient route in terms of energy barriers includes two copper ions. Based on the calculation, the reaction follows a di-copper stepwise mechanism involving the formation of a six-membered ring and then undergoes a ring contraction to a five-membered ring. The regiochemistry of the reaction was investigated based on local and global reactivity indices of reactants, the transition state stabilities calculation. The electron reorganization along the uncatalyzed one-step mechanism has been investigated by the ELF topological analysis of the bonding changes along with the CA reaction.

1. Introduction

One of the most efficient synthetic tools for triazole derivatives' convenient preparation in a regioselective manner is the click reaction [1, 2]. Click reaction proceeds with regioselectivity and has an optimal atom economy, which is influential and crucial in synthetic chemistry [3, 4]. 1,2,3-Triazole scaffolds are utilized for treatment of HIV [5], tumors [6, 7] allergy [8], fungal infection [9, 10] and microbial diseases [11, 12, 13, 14, 15]. Huisgen, introduced uncatalyzed cycloaddition (CA) of alkynes and azides through thermal click reaction, with usually a mixture of 1,4- and 1,5- triazoles products in variable yields [16]. As shown in Scheme 1, Sharpless [17] and Meldal [18] reported the regioselective synthesis of 1,4-disubstituted triazoles through copper catalyzed azide-alkyne CA (CuAAC) reaction, in short time reactions and under mild conditions [19, 20, 21, 22]. The essential Cu(I) species for CuAAC reactions have been added as a cuprous salt with stabilizing ligands [18, 23, 24, 25], or were produced from copper (II) salts by using reducing agents [26]. Recently, several computational studies were presented on the mechanism of click reaction in the presence of different catalyst including Ru, Cu, Mg which results different regioselectivity [19, 27, 28, 29, 30, 31, 32, 33]. On the other

hand, thiazolidinone derivatives have been the subject to considerable studies, because of important biological applications such as antibacterial [34, 35, 36, 37, 38], antiviral [39, 40, 41], antifungal [42, 43, 44] and antituberculosis properties [35, 45, 46].

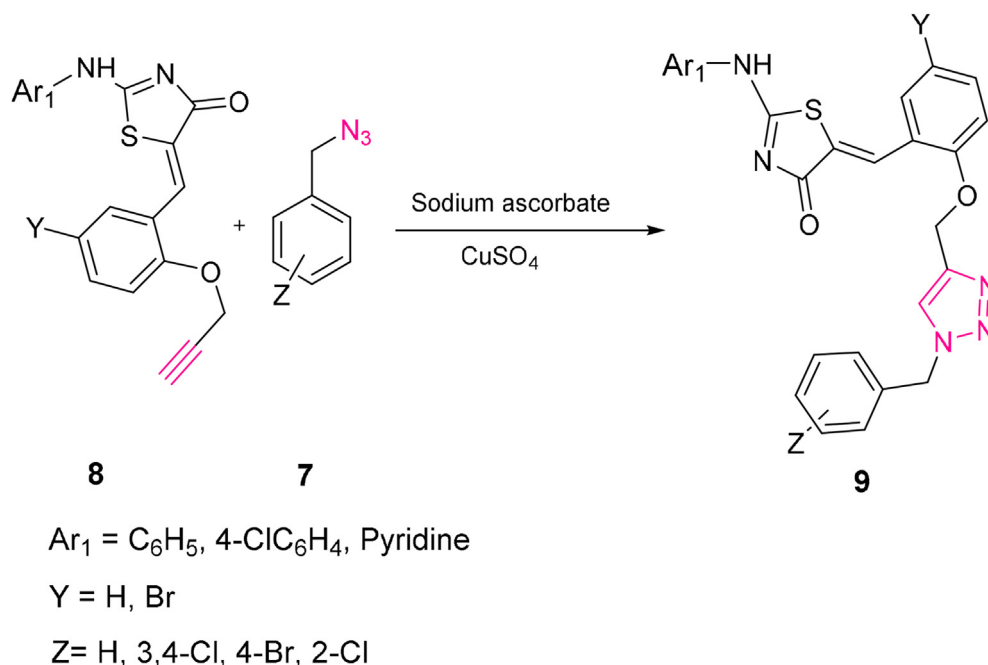
To extend bioactive structures and overwhelm the inherent defects, merging scaffolds and introducing the various functional groups onto the backbone of heterocycles have been considered [47]. Based on the pharmacological properties associated with thiazolidinone and triazole derivatives [19, 48, 49], we were interested in the combine these heterocyclic moieties through click reaction [50, 51, 52]. Therefore, the alkyne fragment was generated through the Knoevenagel condensation of 4-thiazolidinones derivatives with propargylated salicylaldehyde. In the following, the triazole derivatives have been prepared through CuAAC reactions in aqueous/DMSO solution (Scheme 1). Besides, the regioselectivity and mechanism of this CA reaction were studied at B3LYP and wB97XD levels of theory [53]. Accordingly, a theoretical study on the five possible pathways involving the *one-step* mechanism with uncatalyzed, mono-copper and di-copper catalyzed processes. Also, the stepwise di-copper and mono-copper catalyzed mechanism were carried out.

* Corresponding author.

E-mail address: ysarrafi@umz.ac.ir (Y. Sarrafi).<https://doi.org/10.1016/j.heliyon.2021.e06113>

Received 18 May 2020; Received in revised form 23 July 2020; Accepted 26 January 2021

2405-8440/© 2021 Published by Elsevier Ltd. This is an open access article under the CC BY-NC-ND license (<http://creativecommons.org/licenses/by-nc-nd/4.0/>).



Scheme 1. CuAAC reaction between alkyne and benzyl azide.

1.1. Experimental

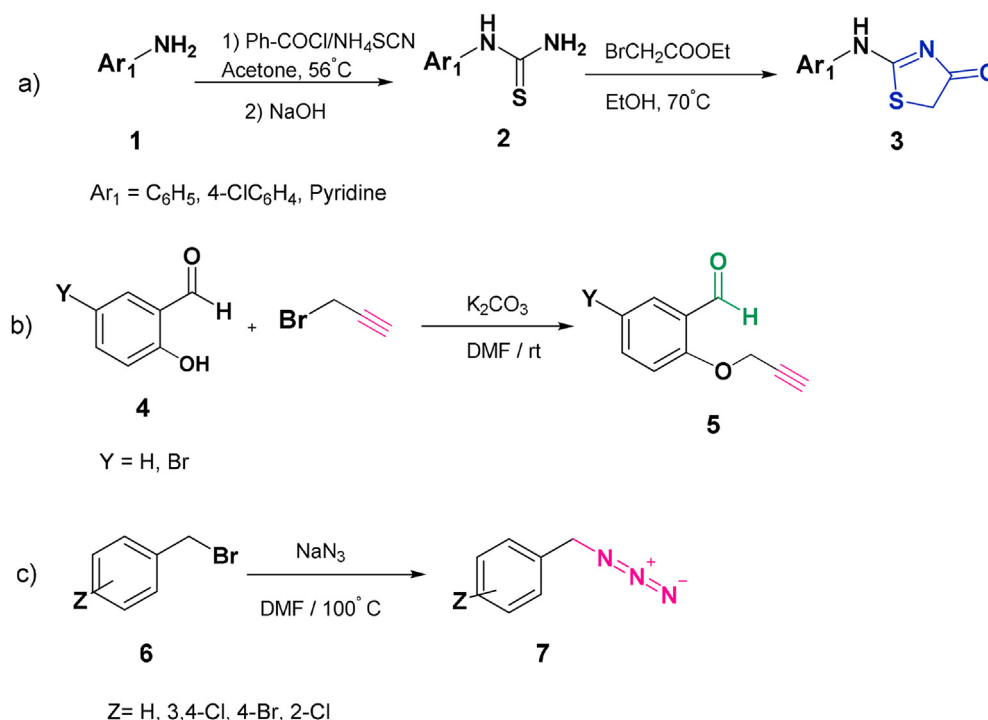
Initially, 5-arylidene-4-thiazolidinone **3** was prepared as the tautomeric mixtures under the literature procedure [54, 55]. Then, compound **5** was synthesized from the propargyl bromide and 2-hydroxy benzaldehyde **4** in the presence of K_2CO_3 [56]. The organic azides preparation procedure is shown in Scheme 2 [57].

The dipolarophiles **8** were synthesized by the reaction of thiazolidinone **3** with propargylated salicylaldehyde **5** and malononitrile as a catalyst under reflux in good yield. Then, dipolarophile **8** was formed through a Michael addition reaction between the active CH_2 group of the

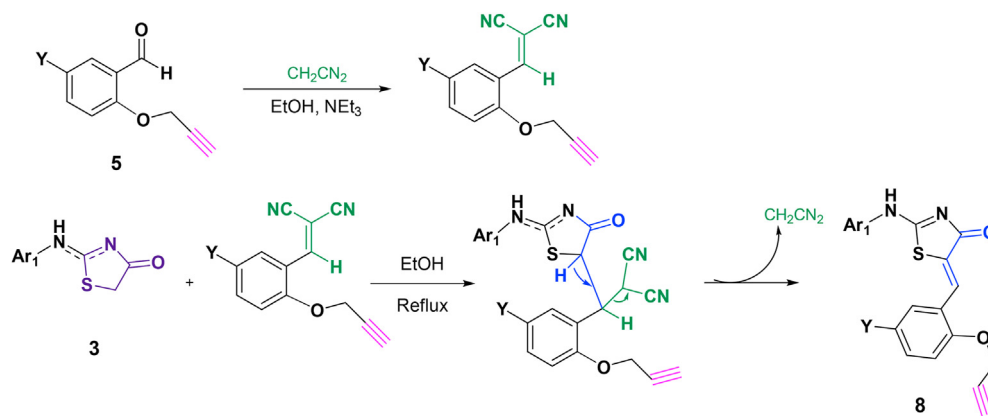
4-thiazolidinones **3** with the $\text{C}=\text{C}$ bond of malononitrile arylidene (Scheme 3) [58,59].

1.2. Computational details

All calculation investigations were performed by DFT theory with wB97XD [61] and B3LYP [60] functionals as implemented in the Gaussian 09 program package [62]. The geometries of all transition states (TSs) and ground states (GSs) were optimized utilizing the LANL2DZ pseudopotential basis set for Cu element and 6-311+G(d,p) basis set for the C, N, H, O elements [60]. Solvent effects were studied



Scheme 2. Preparation of starting materials.



Scheme 3. Synthesis of the alkyne derivatives 8.

using CPCM calculations in the mixed solvents (Water: DMSO) [63, 64, 65, 66, 67, 68, 69]. Based on optimized geometries, single-point (SP) calculations were performed with the full basis set (6-311+G(2d, 2p)) for all elements. Selected reaction pathway for the uncatalyzed scenario was subjected to IRC calculations with the intention of tracing their pathways and confirming that the optimized TS structure connects the accurate reactants and products [70, 71]. The ^1H chemical shift was also investigated through the GIAO method using the TMS as ^1H reference at the B3LYP/6-311+G(2d,2p) level [72]. The Gibbs free energies (G) reported, which include zero-point vibrational corrections (E), entropy (S), and thermal (H) corrections, and solvation energies at 353 K are considered in ΔG . All energies were amended with the SP dispersion effect through the DFT-D2 method [73]. It has revealed that the inclusion of these effects could improve the accuracy of the B3LYP method [74]. The ELF's topological analysis was accomplished with the TopMod program for the uncatalyzed cycloaddition step [75].

2. Results and discussion

2.1. Experiment

In the first endeavor, (Z)-5-(2-((1-benzyl-1H-1,2,3-triazole-4-yl)methoxy)benzylidene)-2-(phenylamino)thiazol-4(5H)-one 9a was prepared from CuAAC reaction of benzyl azide 7a and (Z)-2-(phenylamino)-5-(2-(prop-2-yn-1-yloxy)benzylidene)thiazol-4(5H)-one 8a. The synthetic route is outlined in Scheme 1.

To find optimum conditions to maximize the yields of the 1,2,3-triazoles 9a-h, various solvents were investigated for the CA reaction between 8a and benzyl azide 7a, using CuSO_4 as copper source and sodium ascorbate as reductant (Scheme 1). According to Table 1, the most effective solvent system is the water-DMSO (3:1) system, which is consistent with the previous report by Candelon [25]. This procedure was applied to benzyl azide derivatives and a series of terminal alkynes 8b-h under the same conditions to form triazole products in acceptable yields (Scheme 1).

The active Cu (I) is produced in situ through the reduction of the Cu(II) salt (0.5mol %) with sodium ascorbate. Furthermore, a small extra of sodium ascorbate prevents the coupling reaction that can be observed when a copper (I) source is used directly (Table 1 and 2) [18].

Table 1. Optimizing the CA reaction in order to generate 9a.

Entry	catalyst	Solvent	Yield (%)	Time (h)
1	CuSO_4	DMSO ^a	70	24
2	CuSO_4	DMSO-Water ^a	94	15
3	CuSO_4	Water ^b	65	20

^a 1,4-triazole as a regioselective cycloadducts.

^b a mixture of 1,5- and 1,4- triazole cycloadducts.

As shown in Figure 1, a mixture of tautomeric cycloadducts 9a and 9a' was shown by the cycloaddition reaction in DMSO-Water. Several spectroscopic techniques assigned the structure of the cycloadduct 9a. For the solid products 9a and 9a', the demonstrated absorptions at 3354 cm^{-1} , 1686 cm^{-1} , and 1176 cm^{-1} are ascribed to NH, CO, and ether groups. The NMR spectral data of isolated products were in good agreement with the 9a and 9a's assigned structure. The ^1H NMR spectrum of 9a and 9a' exhibited a singlet at $\delta = 7.90$ for Hd, and two singlet peaks of $-\text{CH}_2$ groups at 5.26 and 5.30 ppm for Ha belong to 9a and 9a', respectively. Two singlet peaks at 8.30 ppm and 8.34 ppm of CH are referred to as methine groups (Hc). Also, two signals at 11.54 and 12.34 ppm for NH protons are evidence for forming a mixture of tautomer's 9a and 9a'. The ^{13}C NMR of 9a displayed two peaks at 53.32 and 62.13 ppm because of the CH_2 group and the attached CH_2 to the oxygen group. The preparation of the cycloadduct 9 was also confirmed by mass spectral data, which exhibited a molecular ion peak at 467.1 (M+). This procedure was applied to a series of organic azides and terminal alkynes under similar conditions to form the corresponding triazole products in good yields.

In 2009, Khoshkholg and coworkers [76] described a one-pot reaction to form 6H-Indeno[2',1':5,6]pyrano[3,4-c]chromen-13(13bH)-one under a CA reaction to give the corresponding pyran. In 2012, Pałasz also reported a multi-component, one-pot reaction for pyrano[2,3-d]pyrimidine derivative synthesis through domino Knoevenagel/Diels-Alder reactions [59]. Accordingly, we had planned the synthesis of N-phenyl-6H,11bH-chromeno [4',3':4,5] pyrano[2,3-d]thiazol-2-amine 12 from an intramolecular hetero Diels-Alder (HAD) reaction of α,β -unsaturated carbonyl compound 8a (Scheme 4). This reaction was investigated under various conditions and solvents, and unfortunately, all attempts to isolate the desired product failed.

The regioselectivity and mechanism of this CuAAC from a computational point of view are investigated utilizing DFT.

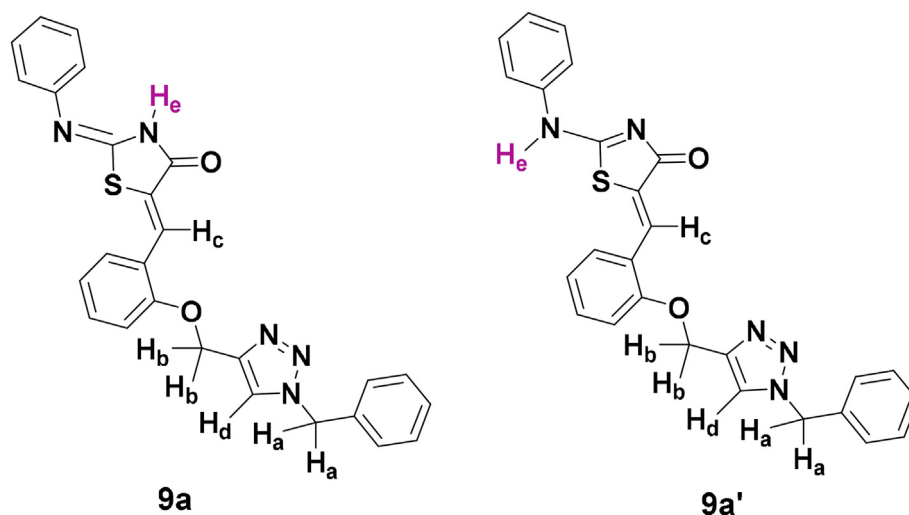
2.2. Computational

2.2.1. Catalyzed vs. uncatalyzed one-step 32CA

Two regioisomeric cycloadducts could be formed in the 32CA reactions of 7a and 8a owing to the asymmetry of reagents. Analysis of the stationary points found in this cycloaddition reaction indicates that it occurs through a one-step mechanism. Consequently, two transition states, Ts-U1 and Ts-U2, and corresponding triazoles 9a and F were characterized. As represented in Figure 2, both regioisomeric paths have high activation free-energy barriers (E_a) in the absence of the copper catalyst. The 32CA reaction path U1 in the cycloadduct 9a that is exergonic by 35.7 kcal/mol has a 39.9 kcal/mol barrier. However, the pathway U2, which leads to cycloadduct D with a more barrier (40.8 kcal/mol), is exergonic by 36.8 kcal/mol. The optimized geometries of the uncatalyzed TSs are shown in Figure 2.

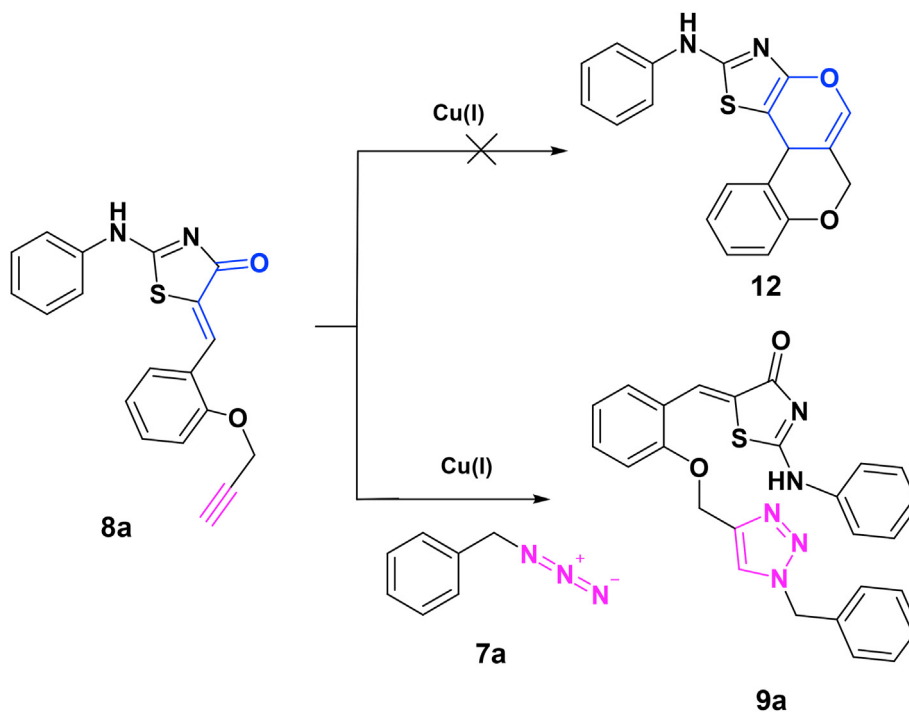
Table 2. Cu-catalyzed 32CA reaction of azide and alkyne.

Entry	X	Y	Z	Yield (%)
9a	H	H	H	95
9b	H	H	3,4-Cl	75
9c	H	H	4-Br	71
9d	Py	H	4-Br	82
9e	Py	H	2-Cl	81
9f	Py	5-Br	H	85
9g	Py	H	3,4-Cl	86
9h	4-Cl	H	2-Cl	58

**Figure 1.** The structures of 9a and 9a'.

The CA reaction of azide **7a** toward alkyne **B** in water as ligand for Cu(I), was investigated utilizing DFT calculations (Figure 3). Study on the stationary points found along the two 1,4- and 1,5-triazole preparation reveals that the proposed cycloaddition reaction through a one-step

mechanism takes place through two transition states **Ts-C1** and **Ts-C2** and the corresponding metallated triazoles **E** and **F**, along with the 1,4- and 1,5-regioisomeric reaction pathways were placed and characterized. As forecast in the absence of the catalyst, the calculated E_a for both

**Scheme 4.** Possible hetero Diels-Alder and click reactions of **8a**.

regioisomers is more than of that the presence of Cu catalyst ($\Delta\Delta G^\ddagger = 11.3$ and 7.8 kcal/mol for Pathways C1 and C2, respectively). Both paths are exergonic, respectively by 4.1 and 5.8 kcal/mol (Scheme 1). The calculations exhibited that the E_a for Pathway C1 is nearly similar to pathway C2 (35.5 and 38.5 kcal/mol, respectively). The intermediate F has a lower barrier, and it is more endergonic (1.7 kcal/mol), which is in agreement with the experimental observations. The optimized geometries of TSs **Ts-C1** and **Ts-C2** are displayed in Figure 3.

In the namely reaction conditions, by coordinating of Cu(L)+alkyne **8a** is considerably acidified. The calculations show that the coordination process is exergonic by 3.1 kcal/mol. The deprotonation process of complex A to acetylide C, using a base in the solvent, is also exergonic by 3.4 kcal/mol, shown in Scheme 5. On the other hand, the overall deprotonation process with two copper ions is exergonic by 6.5 kcal/mol. In intermediate C, one copper ion coordinates the π system, while the other copper is bound to the σ bound of the alkynyl ligand.

The reaction of azide **7a** with alkyne **C** in the presence of two Cu(L) was also calculated through DFT calculations to explain the total regioselectivity experimentally observed (Figure 4). Analysis of the stationary structures found along the two 1,4- and 1,5-regioisomeric reaction pathways indicates that this di-copper *one-step* cycloaddition reaction takes place through two transition states, **Ts-D1** and **Ts-D2** and also the corresponding metallated-triazoles **I** and **L**, along with the 1,4- and 1,5-regioisomeric reaction pathways were characterized. Accordingly, in the presence of two copper ions, both of calculated E_a s

for two different regioisomeric pathways are lower than that of mono-copper and without Cu catalyst pathways, **Ts-D1** (23.5 kcal/mol) and **Ts-D2** (28.3 kcal/mol) < **Ts-C1** (35.5 kcal/mol) < **Ts-C2** (38.5 kcal/mol) < **Ts-U1** (39.9 kcal/mol) < **Ts-U2** (40.8 kcal/mol). In contrast, the pathway DC1, which afford triazole **9a**, has a much lower energy barrier than the second pathway DC2 by 20.4 kcal/mol vs. 25.2 kcal/mol. As well, the intermediate L formation is exergonic by 9.8 kcal/mol. These results are along with the experimentally observed regioselectivity of reaction. The optimized geometries of TSs **Ts-D1** and **Ts-D2** are shown in reaction of azide **7a** with alkyne **C** in the presence of two Cu(L) was also calculated through DFT calculations (Figure 4). These results indicated that the di-copper catalyzed reaction's overall barriers are lower than the mono-copper catalyzed, and that of the mono-copper catalyzed reaction is lower than the uncatalyzed. In the presence of a two-copper, E_a for the formation of the 1,4-triazoles decreases more than the 1,5-triazoles.

For the di-copper case, it is estimated that the favorable product is 1,4-triazole in line with experimental results. In the di-copper pathway, considering weak interactions such as the π/π interactions, **Ts-D1** and **Ts-D2** have the lower energy, and pathway DC1 is more preferred than DC2, which is in accordance with the experimental result (calculation in wB97XD functional). It is worth revealing that more theoretical studies about CA reactions will be efficient to understand the accuracy of wB97XD and B3LYP functionals in the prediction of regioselectivity (Supporting information Table 1).

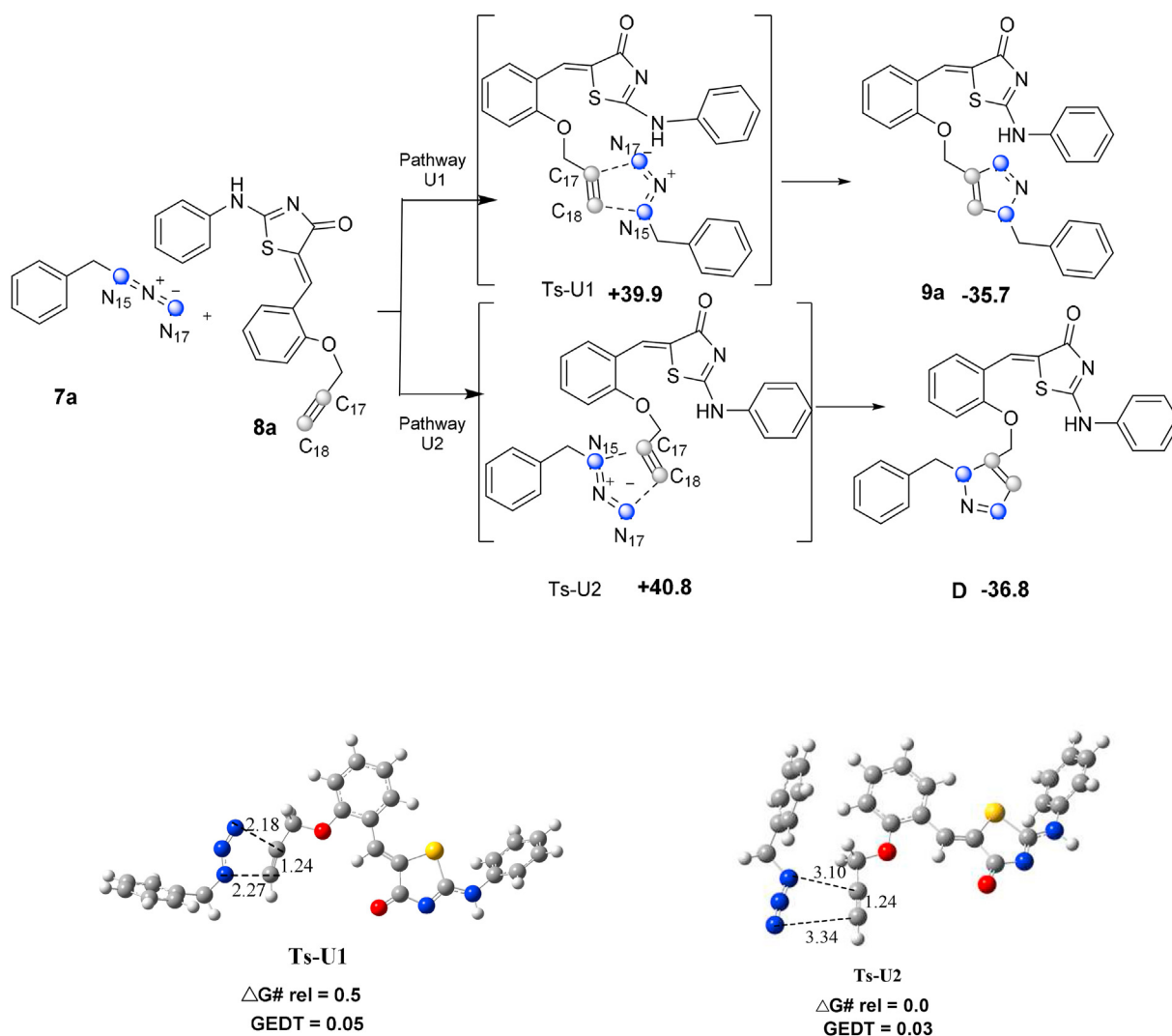


Figure 2. The uncatalyzed CA pathways. Distances in angstroms (Å). Energies are in (kcal/mol).

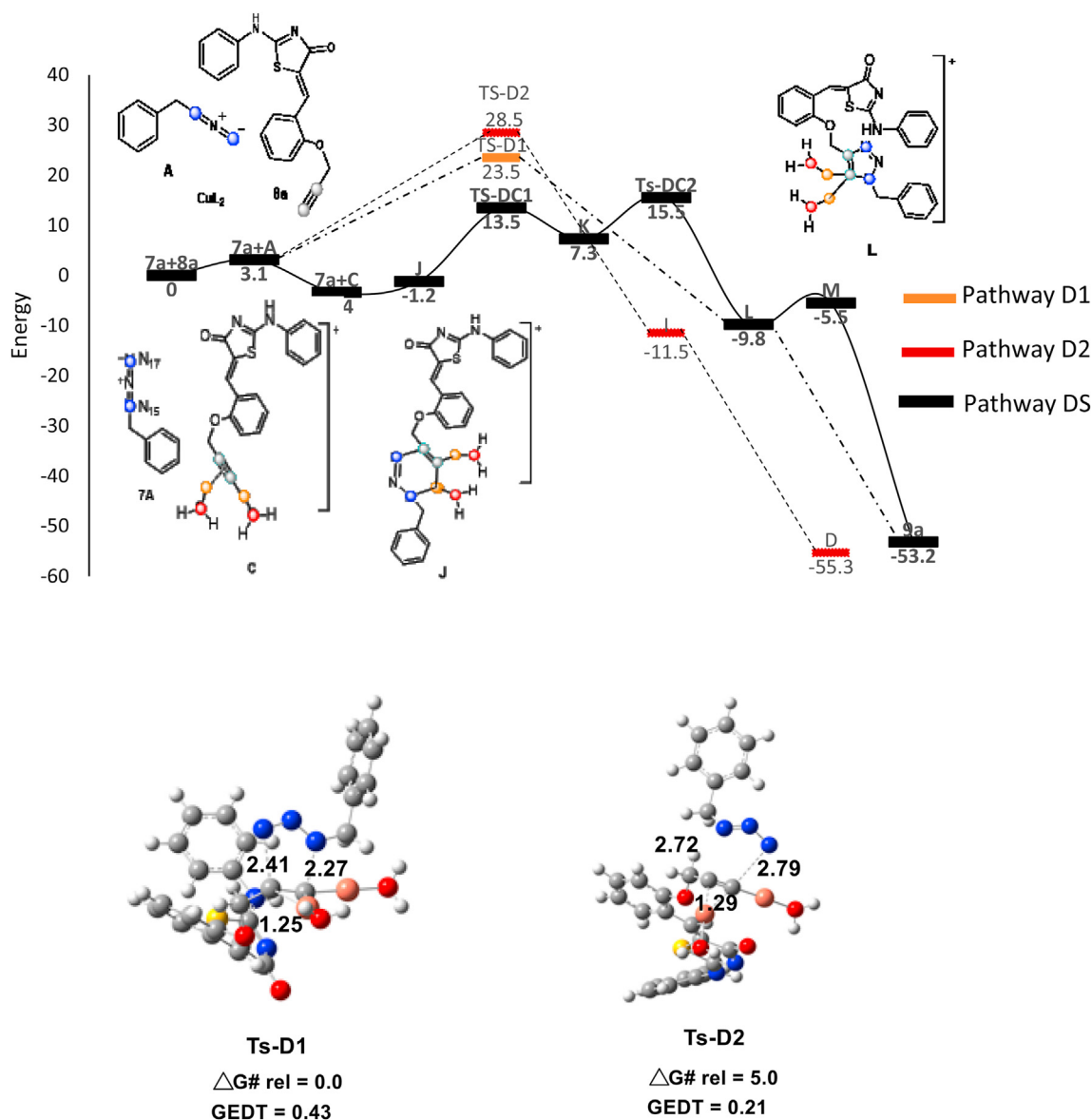


Figure 4. The di-copper catalyzed CA pathways. Distances in angstroms (Å). Energies are in (kcal/mol).

pathway's computed energies predict an exergonic overall reaction ($\Delta G = -53.2$ kcal/mol).

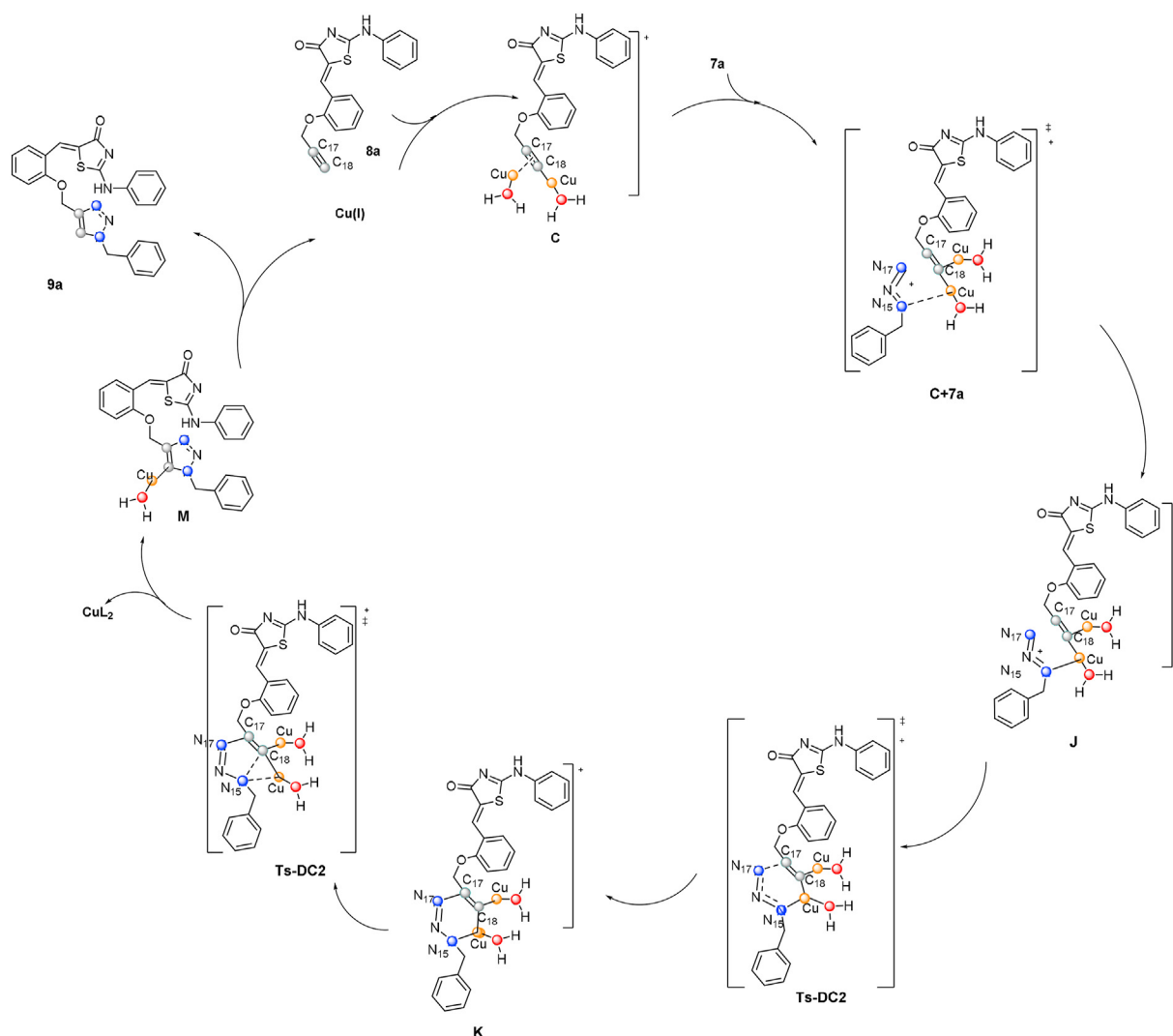
The proposed mechanism, including two Cu ions, is shown in Scheme 6. The Cu-catalyst is contained in each step of the reaction, which efficiently lowers all of them' energy barriers. Primary, Cu coordination raises the alkyne's acidity, facilitating a relatively weak base's deprotonation process. As discussed above, a second Cu ion's involvement in this step makes the deprotonation more comfortable. Second, Cu species allows the CA to occur in a stepwise manner, with much lower energy barriers than those found for the uncatalyzed CA reaction.

Also, a probable mechanism involving one Cu ion was studied in Figure 3. The energy profile for this scenario is considered in a stepwise manner, which is analogous to the one found for the reaction involving two Cu species. This manner was started by C–N bond formation affording a six-membered ring intermediate H, tailed by a ring contraction leading to metallated triazole E. In the mono-copper stepwise pathway SC, intermediate E is formed through Ts-Sc1, an asynchronous transition state with a shorter distance for the C–N bond forming. We also could locate a transition state Ts-Sc2 for the ring contraction of metallated triazole, which would lead to the formation of 1,4-disubstituted triazole 9a. However, all these possibilities have high barriers to be

viable under the experimental reaction conditions. The stepwise mechanism has a 17.4 kcal/mol barrier for Ts-Sc1, while the one-step mechanism C1 has barriers of 30.0, or 36.0 kcal/mol, depending on the regiochemistry of the cycloaddition reaction.

2.2.3. Local and global properties analysis

The regioselectivity of CA could be studied through the global and local indices defined in the DFT context. Global electrophilicity index, which measured the total electron attraction abilities from the environment, is defined as $\omega = \mu^2/(2\eta)$. Chemical hardness (η) is the differences between LUMO (ϵ_L) and HOMO (ϵ_H) energies, and the global softness computed as $S = 1/2\eta$. Electronic chemical potential μ is a relative measure of the molecular capacity to donate electron density, defined the mean value of ϵ_L and ϵ_H as $\mu \sim (\epsilon_H + \epsilon_L)/2$ and the relative global nucleophilicity index N, based on ϵ_H well-defined as $N = \epsilon_{H(Nuc)} - \epsilon_{H(TCE)}$ where TCE is tetracyanoethylene [79, 80, 81, 82]. As presented in Table 3, the static global properties, namely global nucleophilicity N, global electrophilicity ω , chemical hardness η , and electronic chemical potential μ indices of di-copper acetylide C, copper acetylide B, alkyne 8a, and azide 7a are reported. The electrophilicity of alkyne 8a is more significant than azide 7a. The electronic chemical potential of azide 7a is



Scheme 6. The plausible mechanism of di-copper catalyzed stepwise CA.

more significant than alkyne **8a**, representing charge transfer (CT) flux from azide **7a** toward alkyne **8a**. The mono-copper acetylide **B** and dicopper acetylide **C** have higher electronic chemical potential and nucleophilicity than azide **7a** in Table 4, suggesting that along with a polar 32CA reaction, the GEDT can occur from alkynes **B** and **C** to azide **7a**. More to say, in the nucleophilicity scale, the di-copper acetylide **C** being classified as a strong nucleophile because of the high value of nucleophilicity, $N = 4.21$ eV [83].

Overall, the polar character of 32CA was assessed by calculating the GEDT at TSs. In this study, the GEDT [84] was calculated for all the optimized TSs using Natural Population Analysis (NPA) [85, 86], which are given in Figures 2, 3, and 4. Accordingly, the GEDT for Pathways U1 and U2 of the azide **7a** with alkyne **B** reaction is 0.05e and 0.03e, respectively. On the other hand, the GEDT that fluxes from alkynes **B** and **C** towards azide **7a** for Ts-C1, Ts-C2, Ts-DC1, and Ts-DC2 are 0.11e, 0.06e, 0.43e, and 0.21e, respectively. These GEDT values show no polarity character for pathways U1, U2, and C2, whereas pathways C1, DC1, and DC2 are involved in polar 32CAs [85, 86].

By approaching asymmetric nucleophilic/electrophilic pair and a polar process, the most favorable pathway is related to the initial interaction between the most nucleophilic centers of the nucleophile and the most electrophilic centers of the electrophile. Lately, the nucleophilic Parr function Pk^- and electrophilic function Pk^+ are proposed by Domingo et al. as powerful tools to study the local interaction in ionic and polar processes. Pk^+ and Pk^- functions are gained from the atomic spin

density maps (ASD) at the radical cations and the radical anions of the reagents [87, 88], which are powerful tools to study the local interaction in ionic and polar processes [89, 90, 91, 92, 93, 94].

The ASD maps of the radical anions of azide **7a**, alkynes **B**, and **C** and that of the radical cations of azide **7a** and alkyne **8a** are shown in Figure 5. As shown in Table 3, analysis of the nucleophilic and electrophilic functions at the reactive sites of azide **7a** indicates that the N15 ($Pk^- = 0.47$ vs. 0.25) and N17 ($Pk^+ = 0.57$ vs. 0.21) are the most nucleophilic and electrophilic centers, respectively. Alkyne **8a**, without any copper catalyst, has the highest electrophilic activation at the C17 atom. Therefore, it is predictable that the C17 of alkyne **8a** will be the most favored position for a nucleophilic attack of the N15 atom of azide **7a**. The analysis of the ASD maps of mono- and di-copper acetylide **B** and **C** indicate that the C17 has the more extensive nucleophilic activation than C18, so it is predictable that the C17 of alkynes **B** and **C** will be the favored position for a nucleophilic attack to the N17 of azide **7a** which these interactions are in good agreement with the experimental regioselectivity.

2.2.4. ^1H NMR spectral analysis

The use of ^1H -NMR spectroscopy enhanced the characterization of the arylaminothiazol-4-one **3a** and triazole **9a**. The arylaminothiazol-4-one compounds exist as a mixture of tautomeric equilibrium **3a** and **3a'** in DMSO solution; thus, the CA reaction products also include both of the tautomeric cycloadducts **9a** and **9a'**. The evaluation between the

Table 3. Electronics Chemical Potential, μ , Global Electrophilicity, ω , Chemical Hardness, η , and Nucleophilicity index, N in eV, Values of azide 7a, alkyne 8a, B and C.

Structure	Atoms	μ	η	ω	N	S	P_K^-	P_K^+
7a	15	-3.31	5.01	0.96	3.15	0.09	0.47	0.21
	17						0.25	0.57
8a	17	-3.73	7.20	0.98	1.85	0.06	0.20	0.45
	18						0.28	0.23
B	17	-3.42	5.63	1.05	2.88	0.08	0.19	0.10
	18						0.14	0.27
C	17	-2.89	4.01	1.1	4.21	0.12	0.30	0.22
	18						0.19	0.06

calculated chemical shifts and possible products' experimental data could be useful due to a similar splitting pattern for the two tautomeric cycloadducts. Thus, the $^1\text{H-NMR}$ chemical shifts of compounds **3a**, **3a'**, **9a**, and **9a'** were calculated using the GIAO method, and the results were summarized in Table 4. The theoretical values of H_a , H_b , H_c , and H_e of compounds **3a** and **3a'**, as well as **9a** and **9a'** for 32CA reaction, are close to the experimental values.

2.2.5. ELF topological analysis of the mechanism of the uncatalyzed cycloaddition pathway U1

A well-known powerful tool for studying the bonding changes along the organic reactions is ELF [95]. Recent ELF studies revealed that non-polar [96] and polar [97] 32CA reactions occur through the pseudo radical center. Here, the uncatalyzed one-step pathway has been studied by the ELF topological analysis of the bonding changes along with the reaction. The ELF attractors and calculated valence basin populations of selected points of the IRC pathway of U1 are shown in Figure 6. The ELF topological analysis of the attractors at transition state Ts-U1 demonstrates a monosynaptic basin at C17 of azide fragment, at a C17–N17 distance of 2.23 Å, with a population of 0.01e. Then, at C18–N15 distance of 1.98 Å, two monosynaptic basins emerge with the populations of 0.20 e for V(C18) and 1.13 e for V(N15), while the population of V(C17) increased to 0.58e. Consequently, after passing the TS two pseudoradical centers, which are necessary for the formation of the C18–N15 single bond, have been

emerged. Then, the first new C–N single bond is formed through the combination of two monosynaptic basins V(C18) and V(N15) at a C18–N15 distance of 1.70 Å and a disynaptic basin with the integration of 1.81e is created. Along with this point, two monosynaptic basins V(C17) and V(N17) are also observed with populations of 0.72e and 0.66 e, respectively. Finally, at a C17–N17 distance 1.63 Å, a disynaptic V(C17,N17) basin is observed and the triazole ring is formed. A two-stage one-step mechanism characterized this reaction because of the two new single bonds' formations at two differentiated phases of IRC (Figure 6) [84].

3. Discussion

In summary, novel thiazolidinone 1,4-triazole analogs were synthesized through azide-alkyne cycloaddition reaction using click chemistry with a 63–95% yield. The alkynes were synthesized via the Knoevenagel condensation of propargylated salicylaldehyde with 4-thiazolidinones derivatives. The regiochemistry and mechanism of the reaction have been studied in terms of local and global reactivity indices at the B3LYP level of theory. FMO analysis are along with the experimental results. The stepwise mono-copper and di-copper catalyzed cycloaddition mechanisms are also studied. As expected, the di-copper catalyzed stepwise cycloaddition step exhibits a lower E_a than the mono-copper catalyzed stepwise cycloaddition, catalyzed and uncatalyzed one step mechanisms. The DFT-D results have the lowest energy as a result of the π/π interaction

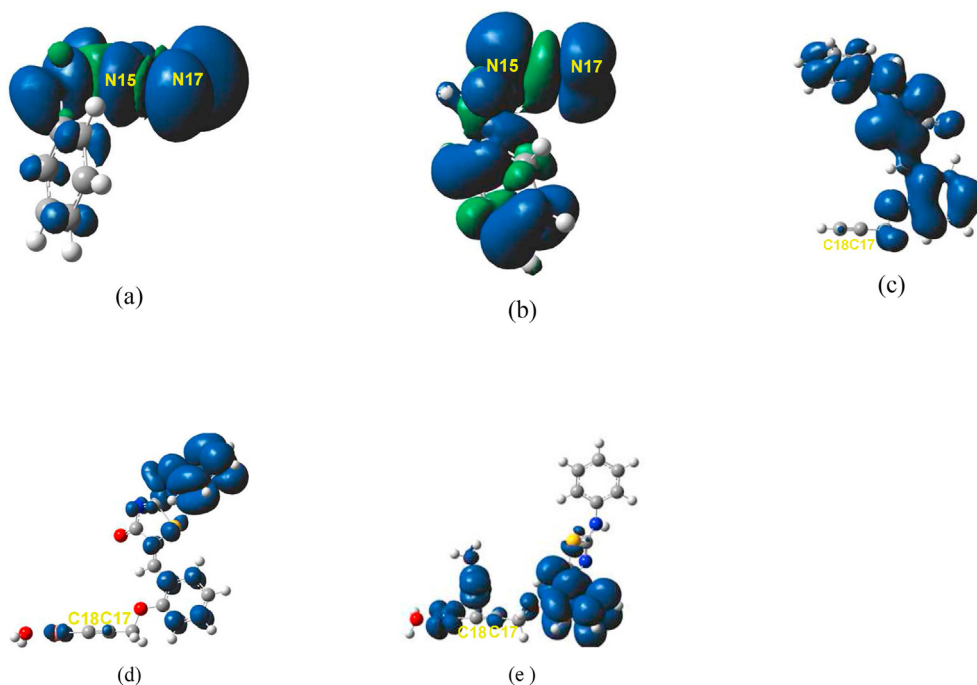
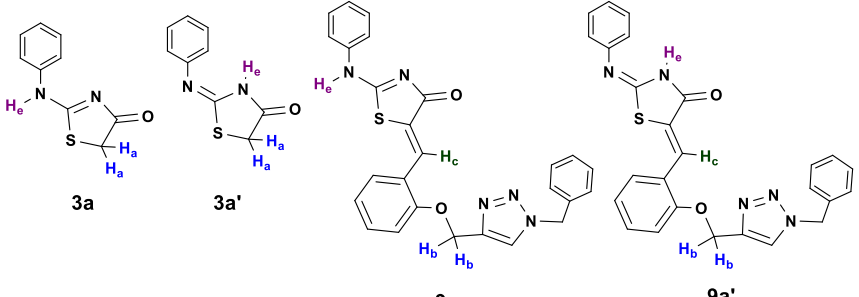
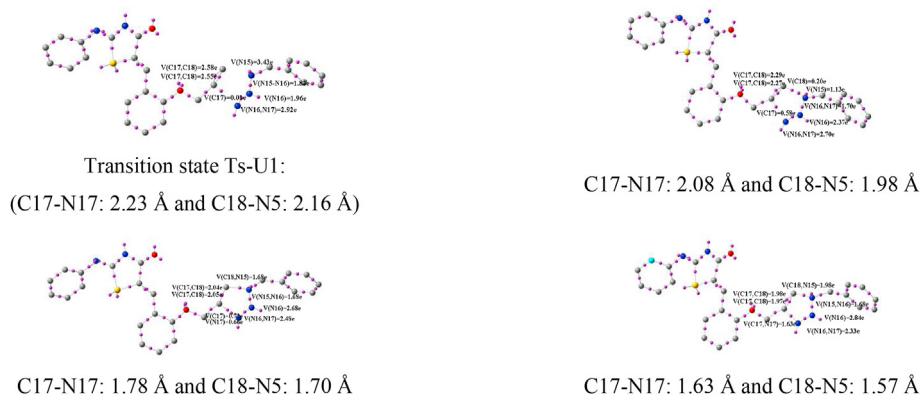


Figure 5. (a) ASD map of the azide radical anion **7a⁻**, (b) the azide radical cation **7a⁺** (c) the alkyne radical cation **8a⁺**, (d) the mono-copper acetylide radical anion **B⁻** and (e) the di-copper acetylide radical anion **C⁻**.

Table 4. Comparison of the theoretical and experimental $^1\text{H-NMR}$ chemical shifts data (δ/ppm) of H_a , H_b , H_c and H_e of each tautomeric cycloadducts.


Atom number	3a	3a'	9a	9a'	Experimental
H_e	11.40	11.57			11.83 11.28
H_a	4.07	4.26			4.01 3.97
H_e			11.80	12.25	12.34 11.54
H_b			5.06	5.23	5.26 5.30
H_c			8.70	8.49	8.34 8.30

**Figure 6.** The calculated ELF valence basins populations of the IRC path of the U1 pathway.

in accordance with the experiment. The calculations show that the inclusion of these effects can significantly upgrade the accuracy of the results. The ELF analysis, performed on the uncatalyzed 32CA reaction, showed the two-stage one-step mechanism in which the formation of the second single bond, C17–N17, takes place when the first single bond, C18–N15, was almost entirely formed, along with the local and global analysis.

Declarations

Author contribution statement

Mahdiah Darroudi: Conceived and designed the experiments; Performed the experiments; Analyzed and interpreted the data; Contributed reagents, Materials, Analysis tools or data; Wrote the paper.

Yaghoob Sarrafi: Contributed reagents, Materials, Analysis tools or data.

Mahshid Hamzehloueian: Conceived and designed the experiments; Analyzed and interpreted the data; Analysis tools or data, Wrote the paper.

Funding statement

This research did not receive any specific grant from funding agencies in the public, commercial, or not-for-profit sectors.

Data availability statement

Data included in article/supplementary material/referenced in article.

Declaration of interests statement

The authors declare no conflict of interest.

Additional information

Supplementary content related to this article has been published online at <https://doi.org/10.1016/j.heliyon.2021.e06113>.

Acknowledgements

The theoretical calculations reported in this paper were carried out at SANCAR, Turkish-German University System, and Nodes of Computational Applications and Research.

References

- Albert Padwa, *1,3-Dipolar Cycloaddition Chemistry*, Wiley-Blackwell, 1986.
- J. Naga Siva Rao, R. Raghunathan, An expedient diastereoselective synthesis of pyrrolidiny spirooxindoles fused to sugar lactone via [3+2] cycloaddition of azomethine ylides, *Tetrahedron Lett.* 53 (2012) 854–858.
- H. Rouh, Y. Liu, N. Katakam, L. Pham, Y.L. Zhu, G. Li, Synthesis of functionalized chromene and chroman derivatives via cesium carbonate promoted formal [4 + 2] annulation of 2'-hydroxychalcones with allenates, *J. Org. Chem.* 83 (2018) 15372–15379.
- Y. Liu, S. Ahmed, X.Y. Qin, H. Rouh, G. Wu, G. Li, B. Jiang, Synthesis of diastereoenriched α -aminomethyl enamines via a brønsted acid-catalyzed asymmetric Aza-Baylis-Hillman reaction of chiral N-phosphonyl imines, *Chem. - An Asian J.* 15 (2020) 1125–1131.
- D.R. Buckle, C.J. Rockell, H. Smith, B.A. Spicer, Studies on 1,2,3-triazoles. 13. (Piperazinylalkoxy) [1]benzopyrano[2,3-d]-1,2,3-triazol-9(1H)-ones with combined H1-antihistamine and mast cell stabilizing properties. *J. Med. Chem.* 29 (1986) 2262–2267.
- R. Alvarez, S. Velazquez, A. San-Felix, S. Aquaro, E. De Clercq, C.-F. Perno, A. Karlsson, J. Balzarini, M.J. Camarasa, 1,2,3-Triazole-[2,5-Bis-O-(tert-butyl)dimethylsilyl]- β -D-ribofuranosyl]-3'-spiro-5''-(4''-amino-1'',2''-oxathiole 2'',2''-dioxide) (TSAO) analogs: synthesis and anti-HIV-1 activity, *J. Med. Chem.* 37 (1994) 4185–4194. (Accessed 15 July 2016).
- F. de C. da Silva, M.C.B.V. de Souza, I.I.P.P. Frugulhetti, H.C. Castro, S.L. de O. Souza, T.M.L. de Souza, D.Q. Rodrigues, A.M.T. Souza, P.A. Abreu, F. Passamani, Synthesis, HIV-RT inhibitory activity and SAR of 1-benzyl-1H-1,2,3-triazole derivatives of carbohydrates, *Eur. J. Med. Chem.* 44 (2009) 373–383.
- J.C. Fung-Tomc, E. Huczko, B. Minassian, D.P. Bonner, In vitro activity of a new oral triazole, BMS-207147 (ER-30346), *Antimicrob. Agents Chemother.* 42 (1998) 313–318. <http://www.ncbi.nlm.nih.gov/pubmed/9527778>. (Accessed 15 July 2016).
- R. Périon, V. Ferrières, M. Isabel García-Moreno, C. Ortiz Mellet, R. Duval, J.M. García Fernández, D. Puyquellec, 1,2,3-Triazoles and related glycoconjugates as new glycosidase inhibitors, *Tetrahedron* 61 (2005) 9118–9128.
- D.J. Anderson, M.R. Barbachyn, D.E. Emmert, S. a Garmon, D.R. Graber, Substituent effects on the antibacterial activity of Nitroben-Carbon-linked (Azolylphenyl) oxazolidinones with expanded activity against the fastidious gram-negative organisms haemophilusinfluenzaeand moraxellacatarhalis, *J. Med. Chem.* 43 (2000) 953–970. (Accessed 15 July 2016).
- M. Hoshino, Effect of 3-Amino-1,2,4-triazole on the experimental production of liver cancer, *Nature* 186 (1960) 174–175.
- A.M. Thompson, A. Blaser, R.F. Anderson, S.S. Shinde, S.G. Franzblau, Z. Ma, W.A. Denny, B.D. Palmer, Synthesis, reduction potentials, and antitubercular activity of ring A/B analogues of the bioreductive synthesis, reduction potentials, and antitubercular activity of ring A/B, *J. Med. Chem.* 52 (2009) 637–645.
- A.K. Jordão, V.F. Ferreira, E.S. Lima, M.C.B.V.B. de Souza, E.C.L.L. Carlos, H.C. Castro, R.B. Geraldo, C.R. Rodrigues, M.C.B. Almeida, A.C. Cunha, Synthesis, antiplatelet and in silico evaluations of novel N-substituted-phenylamino-5-methyl-1H-1,2,3-triazole-4-carbohydrazides, *Bioorg. Med. Chem.* 17 (2009) 3713–3719.
- D.-R. Hou, S. Alam, T.-C. Kuan, M. Ramanathan, T.-P. Lin, M.-S. Hung, 1,2,3-Triazole derivatives as new cannabinoid CB1 receptor antagonists. *Bioorg. Med. Chem. Lett.* 19 (2009) 1022–1025.
- J. Shen, R. Woodward, J.P. Kedenburg, X. Liu, M. Chen, L. Fang, D. Sun, P.G. Wang, Histone deacetylase inhibitors through click chemistry, *J. Med. Chem.* 51 (2008) 7417–7427.
- A. Padwa, *1,3-Dipolar Cycloaddition Chemistry*, Wiley-Blackwell, New York, 1984. <https://www.abebooks.com/9780471083641/3-Dipolar-Cycloaddition-Chemistry-General-Heterocyclic-047108364X/plp>.
- V.V. Rostovtsev, L.G. Green, V.V. Fokin, K.B. Sharpless, A stepwise huisgen cycloaddition process: copper(I)-Catalyzed regioselective “ligation” of azides and terminal alkynes, *Angew. Chemie Int. Ed.* 41 (2002) 2596–2599.
- C.W. Tornøe, C. Christensen, M. Meldal, Peptidotriazoles on solid phase: triazoles by regioselective copper (I)-catalyzed 1,3-dipolar cycloadditions of terminal alkynes to azides, *J. Org. Chem.* 67 (2002) 3057–3064.
- F. Himo, T. Lovell, R. Hilgraf, V.V. Rostovtsev, L. Noodleman, K.B. Sharpless, V.V. Fokin, Copper(I)-catalyzed synthesis of azoles. DFT study predicts unprecedented reactivity and intermediates, *J. Am. Chem. Soc.* 127 (2005) 210–216.
- S. Díez-González, H.C. Kolb, M.G. Finn, K.B. Sharpless, Well-defined copper(i) complexes for Click azide-alkyne cycloaddition reactions: one Click beyond, *Catal. Sci. Technol.* 1 (2011) 166.
- J.E. Hein, V.V. Fokin, Copper-catalyzed azide-alkyne cycloaddition (CuAAC) and beyond: new reactivity of copper(I) acetylides, *Chem. Soc. Rev.* 39 (2010) 1302–1315.
- Z.X. Liu, B. Bin Chen, M.L. Liu, H.Y. Zou, C.Z. Huang, Cu(I)-doped carbon quantum dots with zigzag edge structure for high efficient catalysis of azide-alkyne cycloadditions, *Green Chem.* 46 (2017) 6473–6475.
- T.R. Chan, R. Hilgraf, K.B. Sharpless, V. V Fokin, Polytriazoles as copper(I)-stabilizing ligands in catalysis, *Org. Lett.* 6 (2004) 2853–2855.
- S. Díez-González, A. Correa, L. Cavallo, S.P. Nolan, (NHC)Copper(I)-Catalyzed [3+2] cycloaddition of azides and mono- or disubstituted alkynes, *Chem. Eur. J.* 12 (2006) 7558–7564.
- N. Candelon, D. Lastécouères, A.K. Diallo, J. Ruiz Aranzas, D. Astruc, A highly active and reusable copper(i)-tren catalyst for the “click” 1,3-dipolar cycloaddition of azides and alkynes, *Chem. Commun.* 41 (2008) 741–743.
- V.V. Rostovtsev, L.G. Green, V.V. Fokin, K.B. Sharpless, A stepwise huisgen cycloaddition process: copper(I)-Catalyzed regioselective “ligation” of azides and terminal alkynes, *Angew. Chem. Int. Ed.* 41 (2002) 2596–2599.
- D. Ikhlef, C. Wang, S. Kahlal, B. Maouche, D. Astruc, J.Y. Saillard, Reaction mechanisms of transition-metal-catalyzed azide-alkyne cycloaddition “click” reactions: a DFT investigation, *Comput. Theor. Chem.* 1073 (2015) 131–138.
- T. Hosseinejad, B. Fattahi, M.M. Heravi, Computational studies on the regioselectivity of metal-catalyzed synthesis of 1,2,3 triazoles via click reaction: a review, *J. Mol. Model.* 21 (2015) 1–37.
- Y. Özkılıç, N.S. Tüzün, A DFT study on the binuclear CuAAC reaction: mechanism in light of new experiments, *Organometallics* 35 (2016) 2589–2599.
- E. Boz, N.Ş. Tüzün, Reaction mechanism of ruthenium-catalyzed azide-alkyne cycloaddition reaction: a DFT study, *J. Organomet. Chem.* 724 (2013) 167–176.
- T. Hosseinejad, M. Dinyari, Computational study on stereoselective synthesis of substituted 1H-tetrazoles via a click reaction: DFT and QTAIM approaches, *Comput. Theor. Chem.* 1071 (2015) 53–60.
- L.R. Domingo, N. Acharjee, A molecular electron density theory study of the Grignard reagent-mediated regioselective direct synthesis of 1,5-disubstituted-1,2,3-triazoles, *J. Phys. Org. Chem.* 33 (2020).
- M. Meldal, F. Diness, Recent fascinating aspects of the CuAAC click reaction, *Trends Chem.* 2 (2020) 569–584.
- C.G. Bonde, N.J. Gaikwad, Synthesis and preliminary evaluation of some pyrazine containing thiazolines and thiazolidinones as antimicrobial agents, *Bioorg. Med. Chem.* 12 (2004) 2151–2161.
- S.G. Kucukguzel, E.E. Oruc, S. Rollas, F. Sahin, A. Ozbek, Synthesis, characterisation and biological activity of novel 4-thiazolidinones, 1, 3, 4-oxadiazoles and some related compounds, *Eur. J. Med. Chem.* 37 (2002) 197–206. <http://www.sciencedirect.com/science/article/pii/S0223523401013265>. (Accessed 4 September 2016).
- A. Croatia, G. Hrvatske, *Acta medica Vol 67 Supl 1 WEB. Pdf, Acta Medica Cordoba* 67 (2013). <http://paperzz.com/doc/5154181/acta-medica-vol-67-supl-1-web.pdf>. (Accessed 4 September 2016).
- Ö. Ateş, H. Altıntaş, G. Ötük, Synthesis and antimicrobial activity of 4-carbomethoxymethyl-2-thiazoles and 5-Nonsubstituted/substituted 2-[(4-Carbomethoxymethylthiazol-2-yl), *Arzneimittelforschung* 50 (2000) 569–575. <http://www.thieme-connect.com/products/ejournals/abstract/10.1055/s-0031-1300251>. (Accessed 4 September 2016).
- O. Ateş, A. Kocabalkanli, G. Saniş, A. Ekinci, Synthesis and antibacterial activity of 5-aryl-2-[(alpha-chloro-alpha-phenylacetyl)/alpha-bromopropionyl] amino]-1, 3, 4-oxadiazoles and 2-[(5-aryl-1, 3, 4-oxadiazol-2-yl) imino]-5-phenyl/methyl-4-thiazolidinone s, *Arzneimittel-forschung* 47 (1997) 1134–1138. <http://europepmc.org/abstract/med/9368708>. (Accessed 4 September 2016).
- A. Rao, A. Carbone, A. Chimirri, E. De Clercq, A.M. Monforte, P. Monforte, C. Pannecouque, M. Zappalà, Synthesis and anti-HIV activity of 2,3-diaryl-1,3-thiazolidin-4-(thi)one derivatives, *Farm* 57 (2002) 747–751.
- M.L. Barreca, A. Chimirri, L. De Luca, A.M. Monforte, P. Monforte, A. Rao, M. Zappal, J. Balzarini, E. De Clercq, C. Pannecouque, M. Witvrouw, Discovery of 2,3-diaryl-1,3-thiazolidin-4-ones as potent anti-HIV-1 agents, *Bioorg. Med. Chem. Lett.* 11 (2001) 1793–1796.
- A. Rao, J. Balzarini, A. Carbone, A. Chimirri, E. De Clercq, A.M. Monforte, P. Monforte, C. Pannecouque, M. Zappalà, Synthesis of new 2,3-diaryl-1,3-thiazolidin-4-ones as anti-HIV agents, *Farmaco* 59 (2004) 33–39.
- H.T. Fahmy, Synthesis of some new triazoles as potential antifungal agents, *Boll. Chim. Farm.* 140 (2000) 422–427. <http://www.ncbi.nlm.nih.gov/pubmed/11822232>. (Accessed 4 September 2016).
- N. Karali, E. İllhan, A. Gürsoy, M. Kiraz, New cyclohexylidenehydrazide and 4-aza-1-thiaspiro[4.5]decan-3-one derivatives of 3-phenyl-4(3H)-quinazolinones, *Farm* 53 (1998) 346–349.
- N. Cesur, Z. Cesur, N. Ergenc, M. Uzun, Synthesis and Antifungal Activity of Some 2-Aryl-3-substituted 4-Thiazolidinones. Synthese und antimykotische Aktivität einiger 2-Aryl-3-substituierter 4-, *Arch. Plus* 327 (1994) 271–272. (Accessed 4 September 2016).
- K. Babaoglu, M.A. Page, V.C. Jones, M.R. McNeil, C. Dong, J.H. Naismith, R.E. Lee, Novel inhibitors of an emerging target in Mycobacterium tuberculosis; substituted thiazolidinones as inhibitors of dTDP-rhamnose synthesis, *Bioorganic & medicinal chemistry letters* 13 (19) (2003) 3227–3230.
- N. Ulusoy, Synthesis and antituberculosis activity of cycloalkylidenehydrazide and 4-aza-1-thiaspiro[4.5]decan-3-one derivatives of imidazo[2,1-b]thiazole, *Arzneimittelforschung* 52 (2002) 565–571. <https://www.thieme-connect.com/products/ejournals/abstract/10.1055/s-0031-1299931>. (Accessed 4 September 2016).
- Q. Chen, H. Yu, L. Wang, Z. ul Abdin, Y. Chen, J. Wang, W. Zhou, X. Yang, R.U. Khan, H. Zhang, X. Chen, Recent progress in chemical modification of starch and its applications, *RSC Adv.* 5 (2015) 67459–67474.
- B.C. Boren, S. Narayan, L.K. Rasmussen, L. Zhang, H. Zhao, Z. Lin, G. Jia, V.V. Fokin, Ruthenium-catalyzed azide-alkyne cycloaddition: scope and mechanism, *J. Am. Chem. Soc.* 130 (2008) 8923–8930.

- [49] D. Cantillo, M. Ávalos, R. Babiano, P. Cintas, J.L. Jiménez, J.C. Palacios, Assessing the whole range of CuAAC mechanisms by DFT calculations—on the intermediacy of copper acetylides, *Org. Biomol. Chem.* 9 (2011) 2952.
- [50] M. Darroudi, S. Ranjbar, M. Esfandiari, M. Khoshneviszadeh, M. Hamzehloueian, M. Khoshneviszadeh, Y. Sarrafi, Synthesis of novel triazole incorporated thiazolone motifs having promising antityrosinase activity through green nanocatalyst CuI-Fe 3 O 4 @SiO 2 (TMS-EDTA), *Appl. Organomet. Chem.* (2020).
- [51] S. Ranjbar, P. Shahvaran, N. Edraki, M. Khoshneviszadeh, M. Darroudi, Y. Sarrafi, M. Hamzehloueian, M. Khoshneviszadeh, 1,2,3-Triazole-linked 5-benzylidene (thio)barbiturates as novel tyrosinase inhibitors and free-radical scavengers, *Arch. Pharm. (Weinheim)* (2020).
- [52] M. Darroudi, Y. Sarrafi, M. Hamzehloueian, An efficient synthesis of novel triazoles incorporating barbituric motifs via [3+2] cycloaddition reaction: experimental and theoretical study, *J. Serb. Chem. Soc.* 83 (2018) 821–835.
- [53] M. Darroudi, Y. Sarrafi, M. Hamzehloueian, Theoretical exploration of mechanism of carbenam formation in catalytic Kinugasa reaction, *Tetrahedron* 73 (2017) 1673–1681.
- [54] H. Behbehani, H.M. Ibrahim, 4-Thiazolidinones in heterocyclic synthesis: synthesis of novel enamines, azolopyrimidines and 2-arylimino-5-arylidene-4-thiazolidinones, *Molecules* 17 (2012) 6362–6385.
- [55] H. Behbehani, H. Ibrahim, S. Makhseed, Studies with 3-oxoalkanonitriles: synthesis and reactivity of 3-Oxo-3-(1-methylindolyl) propanenitrile, *Heterocycles* 78 (2009) 3081–3090. <http://ci.nii.ac.jp/naid/40016842016/>. (Accessed 5 September 2016).
- [56] G. Bashiardes, I. Safir, F. Barbot, J. Laduranty, An expedient synthesis of diversified pyrrolizines and indolizines, *Tetrahedron Lett.* 45 (2004) 1567–1570.
- [57] Y. Kitamura, K. Taniguchi, T. Maegawa, Y. Monguchi, Y. Kitade, H. Sajiki, Copper/HP20: novel and polymer-supported copper catalyst for huisgen cycloaddition. *Heterocycles* 77 (2009) 521–532.
- [58] H. Behbehani, H.M. Ibrahim, S. Makhseed, M.H. Elnagdi, H. Mahmoud, 2-Aminothiophenes as building blocks in heterocyclic synthesis: synthesis and antimicrobial evaluation of a new class of pyrido[1,2-a]thieno[3,2-e]pyrimidine, quinoline and pyridin-2-one derivatives, *Eur. J. Med. Chem.* 52 (2012) 51–65.
- [59] A. Palasz, Synthesis of fused uracils: pyrano[2,3-d]pyrimidines and 1,4-bis(pyran-2,3-d]pyrimidinyl)benzenes by domino Knoevenagel/Diels-Alder reactions, *Monatshfte Für Chemie - Chem. Mon* 143 (2012) 1175–1185.
- [60] P.J. Hay, W.R. Wadt, Ab initio effective core potentials for molecular calculations. Potentials for the transition metal atoms Sc to Hg, *J. Chem. Phys.* 82 (1985) 270.
- [61] J. Da Chai, M. Head-Gordon, Systematic optimization of long-range corrected hybrid density functionals, *J. Chem. Phys.* 128 (2008) 84106.
- [62] M. Robert, 40 sleep hacks, *Fhijfd* 11 (1990) 79–170.
- [63] W.S. MacGregor, The chemical and physical properties of DMSO, *Ann. N. Y. Acad. Sci.* 141 (1967) 3–12.
- [64] A. Luzar, J. Stefan, Dielectric behaviour of DMSO-water mixtures. A hydrogen-bonding model, *J. Mol. Liq.* 46 (1990) 221–238.
- [65] Q. Jie, J. Guo-Zhu, Dielectric constant of polyhydric alcohol-DMSO mixture solution at the microwave frequency, *J. Phys. Chem.* 117 (2013) 12983–12989.
- [66] A. Klamt, G. Schüürmann, COSMO: a new approach to dielectric screening in solvents with explicit expressions for the screening energy and its gradient, *J. Chem. Soc., Perkin Trans. 2* (1993) 799–805.
- [67] J. Andzelm, C. Kölmel, A. Klamt, Incorporation of solvent effects into density functional calculations of molecular energies and geometries, *J. Chem. Phys.* 103 (1995) 9312.
- [68] V. Barone, M. Cossi, Quantum calculation of molecular energies and energy gradients in solution by a conductor solvent model, *J. Phys. Chem.* 102 (1998) 1995–2001.
- [69] M. Cossi, N. Rega, G. Scalmani, V. Barone, Energies, structures, and electronic properties of molecules in solution with the C-PCM solvation model, *J. Comput. Chem.* 24 (2003) 669–681.
- [70] C. Gonzalez, H.B. Schlegel, An improved algorithm for reaction path following, *J. Chem. Phys.* 90 (1989) 2154.
- [71] C. Gonzalez, H.B. Schlegel, Reaction path following in mass-weighted internal coordinates, *J. Phys. Chem.* 94 (1990) 5523–5527.
- [72] K. Wolinski, J. Hinton, P. Pulay, Efficient implementation of the gauge-independent atomic orbital method for NMR chemical shift calculations, *J. Am. Chem.* 112 (1990) 8251–8260. (Accessed 30 September 2016).
- [73] S. Grimme, Semiempirical GGA-type density functional constructed with a long-range dispersion correction, *J. Comput. Chem.* 27 (2006) 1787–1799.
- [74] X. Xu, P. Liu, A. Lesser, L.E. Sirois, P.A. Wender, K.N. Houk, Ligand effects on rates and regioselectivities of Rh(I)-catalyzed (5 + 2) cycloadditions: a computational study of cyclooctadiene and dinaphthocyclooctatetraene as ligands, *J. Am. Chem. Soc.* 134 (2012) 11012–11025.
- [75] A.D. Becke, K.E. Edgecombe, A simple measure of electron localization in atomic and molecular systems, *J. Chem. Phys.* 92 (1990) 5397.
- [76] M. Khoshkholgh, S. Balalaie, H. Bijanzadeh, Intramolecular domino-Knoevenagel-hetero-Diels-Alder reaction with terminal acetylenes, *Arkivoc* 9 (2009) 114–121. https://www.researchgate.net/profile/Hamid_Bijanzadeh/publication/267723170_Intramolecular_domino-Knoevenagel-hetero-Diels-Alder_reaction_with_terminal_acetylenes/links/54b4be570cf28be92e48263.pdf. (Accessed 29 September 2016).
- [77] H.C. Kolb, M.G. Finn, K.B. Sharpless, Click chemistry: diverse chemical function from a few good reactions, *Angew. Chem. Int. Ed.* 40 (2001) 2004–2021.
- [78] V.O. Rodionov, V.V. Fokin, M.G. Finn, Mechanism of the ligand-free CuI-catalyzed azide-alkyne cycloaddition reaction, *angew. Chemie* 117 (2005) 2250–2255.
- [79] M. Rahm, T. Brinck, Novel 1,3-dipolar cycloadditions of dinitramine acid: implications for the chemical stability of ammonium dinitramide, *J. Phys. Chem.* 112 (2008) 2456–2463.
- [80] K.V. Gothelf, K.A. Jørgensen, Asymmetric 1,3-dipolar cycloaddition reactions, *Chem. Rev.* 98 (1998) 863–910.
- [81] D.M. Andrada, A.M. Granados, M. Solà, I. Fernández, DFT study of thermal 1,3-dipolar cycloaddition reactions between alkynyl metal(0) Fischer carbene complexes and 3 H-1,2-dithiole-3-thione derivatives, *Organometallics* 30 (2011) 466–476.
- [82] Z. Chen, L. Lin, M. Wang, X. Liu, X. Feng, Asymmetric synthesis of trans- γ -lactams by a Kinugasa reaction on water, *Chem. Eur. J.* 19 (2013) 7561–7567.
- [83] P. Jaramillo, L.R. Domingo, E. Chamorro, P. Pérez, A further exploration of a nucleophilicity index based on the gas-phase ionization potentials, *J. Mol. Struct. THEOCHEM* 865 (2008) 68–72.
- [84] L.R. Domingo, A new C–C bond formation model based on the quantum chemical topology of electron density, *RSC Adv.* 4 (2014) 32415.
- [85] L.R. Domingo, J.A. Sáez, Understanding the mechanism of polar Diels–Alder reactions, *Org. Biomol. Chem.* 7 (2009) 3576.
- [86] A.E. Reed, R.B. Weinstock, F. Weinhold, Natural population analysis, *J. Chem. Phys.* 83 (1985) 735.
- [87] R.G. Parr, R.G. Pearson, Absolute hardness: companion parameter to absolute electronegativity, *J. Am. Chem. Soc.* 105 (1983) 7512–7516.
- [88] W. Parr, R.G. Yang, Density-functional theory of atoms and molecules. *Int. J. Quant. Chem.* 47 (1993) 101.
- [89] L.R. Domingo, P. Pérez, H.G. Viehe, R. Merenyi, L. Stella, Z. Janousek, R. Sustmann, Global and local reactivity indices for electrophilic/nucleophilic free radicals, *Org. Biomol. Chem.* 11 (2013) 4350.
- [90] L.R. Domingo, M. Arnó, R. Contreras, P. Pérez, Density functional theory study for the cycloaddition of 1,3-butadienes with dimethyl acetylenedicarboxylate. Polar stepwise vs concerted mechanisms, *J. Phys. Chem.* 106 (2002) 952–961.
- [91] L.R. Domingo, A density functional theory study for the Diels–Alder reaction between N-acyl-1-aza-1,3-butadienes and vinylamines. Lewis acid catalyst and solvent effects, *Tetrahedron* 58 (2002) 3765–3774.
- [92] L.R. Domingo, M. José Aurell, Density functional theory study of the cycloaddition reaction of furan derivatives with masked o-benzoquinones. Does the furan act as a dienophile in the cycloaddition reaction? *J. Org. Chem.* 67 (2002) 959–965.
- [93] L.R. Domingo, M. José Aurell, P. Pérez, R. Contreras, Origin of the synchronicity on the transition structures of polar Diels–Alder reactions. Are these reactions [4 + 2] processes? *J. Org. Chem.* 68 (2003) 3884–3890.
- [94] L.R. Domingo, J. Andrés, Enhancing reactivity of carbonyl compounds via hydrogen-bond formation. A DFT study of the hetero-Diels–Alder reaction between butadiene derivative and acetone in chloroform, *J. Org. Chem.* 68 (2003) 8662–8668.
- [95] A. Savin, The electron localization function (ELF) and its relatives: interpretations and difficulties, *J. Mol. Struct. THEOCHEM* 727 (2005) 127–131.
- [96] L.R. Domingo, J.A. Sáez, Understanding the electronic reorganization along the nonpolar [3 + 2] cycloaddition reactions of carbonyl ylides. *J. Org. Chem.* 76 (2011) 373–379.
- [97] L.R. Domingo, E. Chamorro, P. Perez, Understanding the high reactivity of the azomethine ylides in [3 + 2] cycloaddition reactions, *Lett. Org. Chem.* 7 (2010) 432–439.